Estimating the number of fiber orientations in diffusion MRI voxels: a constrained spherical deconvolution study

B. Jeurissen[1], A. Leemans[2], J-D. Tournier[3], D. K. Jones[4], and J. Sijbers[1]
[1]Visionlab, University of Antwerp, Antwerp, Belgium, [2]Image Sciences Institute, University Medical Center Utrecht, Utrecht, Netherlands, [3]Brain Research Institute, Florey Neuroscience Institutes (Austin), Melbourne, Victoria, Australia, [4]CUBRIC, School of Psychology, Cardiff University, Cardiff, United Kingdom

Introduction: It has long been recognized that the Gaussian diffusion tensor model is inappropriate for voxels with complex fiber architecture [1, 2]. Many groups have tried to classify voxels in terms of their diffusion complexity. The earliest studies distinguished between voxels with isotropic, single-fiber anisotropic, and multi-fiber anisotropic complexity and have reported clustered and symmetric regions of increased complexity, supporting genuine effects consistent with anatomical knowledge [3, 4]. However, they were not able to report the number of fiber orientations found in each voxel. Recent advances of high angular resolution diffusion imaging allow the extraction of multiple fiber orientations [5] and have spawned an interest for classification of voxels by the number of fiber orientations. Recently, a Bayesian Automatic Relevance Determination method was proposed to infer the number of fiber orientations in a multi-compartment model [6]. The study was able to find voxels with up to two fiber orientations and estimated the proportion of white matter fiber voxels that contain complex fiber architecture at approximately one third. In this work, we estimated the number of fiber orientations within each voxel using the constrained spherical deconvolution (CSD) method [7] with the residual bootstrap approach [8]. We showed that multiple-fiber profiles arise consistently in various regions of the human brain where complex tissue structure is known to exist. Moreover, we detect voxels with more than two fiber orientations and detect a much higher proportion of multi-fiber voxels than previously reported.

Methods: Acquisition: A healthy subject was scanned 15 times on a 3 Tesla scanner (voxel size: 2.4×2.4×2.4 mm³; 30 gradient directions, 3 B0 images; b-value: 1200 s/mm²). The signal-to-noise ratio (SNR) in the individual B0 images was approximately 25. All scans were concatenated (*not* averaged) into a single 'big' data set and, subsequently, corrected for subject motion and potential eddy-current induced geometrical distortions with the required B-matrix adjustments [9], resulting in a total of 450 *unique* diffusion weighted (DW) and 45 B0 images. Simulations: DW data from voxels with multiple (2 and 3) fiber orientations were simulated by combining the signal from weighted diffusion tensor profiles ([1.7 0.2 0.2]×10^{-3} mm²/s [5]) at angles ranging from 90° to 10° and using *the same* SNR, gradient directions and b-value as in the real data acquisition. This procedure was repeated for N = 1000 Rician noise instances. From these noisy simulated data, the number of fiber orientations was estimated N times as follows. First, the fiber orientation distribution (FOD) was calculated for each voxel using CSD (l_{max} = 8) [6]. Then, a Newton optimization procedure was started from a dense set of equally distributed spherical sample points to find the local maxima of the FOD. Finally, the number of *unique* peak FOD orientations with amplitude greater than a fixed threshold was counted and assumed to be equal to the number of fiber orientations. Different FOD amplitude thresholds were tested and the specificity of the method was calculated by dividing the number of correct orientation counts by N. Experimental data: All voxels belonging to the CSF mask were excluded from the study ('Otsu segmentation' on MD images [10]). N_b = 100 residual bootstrap realizations (spherical harmonics model, l_{max} = 8) of the entire dataset were generated. The number of fiber orientations in each voxel was estimated N_b times as explained above and the most common orientation count was selected as the final orientation count. To measure the reproducibility of the method, the percentage of estimates equal to the most likely estimate was also determined. The results were visualized with the diffusion MRI toolbox *ExploreDTI* [11].

Results: An FOD threshold of 0.1 resulted in the highest specificity and was used for further analysis. Fig. 1 shows the specificity at FOD threshold 0.1 derived from the simulations of two fiber orientations at different angles and relative orientation weights 'w' (similar results for three-fiber orientations, but not shown). Fig. 2 shows the FODs in a region with multiple fiber orientations. Notice how the small peak orientations are still coherent, showing continuous transitions with other surrounding orientations. Fig. 3 plots the (RGB-color coded) orientations detected by the algorithm. Fig. 4 shows the CSF mask that was used to exclude CSF voxels for further analysis. Fig. 5 shows the number of fiber orientations detected in each voxel (red: 1; green: 2; blue: >2). For each voxel, this number was the same in more than 90 out of 100 residual bootstrap realizations, highlighting the reproducibility of the orientation counts at the FOD threshold of 0.1. One-, two- and more-than-two-fiber orientations were found in 5, 25 and 70 % of all non-CSF voxels respectively, highlighting the extent of complex fiber orientation voxels. Restricting the study to all voxels with FA > 0.1, the percentages were 6, 25 and 69 respectively. To completely exclude gray matter voxels, we also applied FA thresholds of 0.2 and 0.3, resulting in 9, 43 and 48 %, and 14, 62 and 24 %, respectively. Fig. 6 shows the single orientation voxels color coded for FOD peak orientation. Fig. 7 shows the double orientation voxels color coded for the primary (a-b) and the secondary peak orientation (c-d). Notice how the fiber orientations in Fig. 6-7 are very clustered and symmetrical, supporting genuine anatomical features. Fig. 8 shows the triple orientation voxels color coded for the primary (a-b), secondary (c-d) and tertiary peak orientation (e-f). Notice that, while the primary orientations are still strongly clustered, the clustering decreases for the secondary and tertiary orientations. This is due to the sorting of the secondary and tertiary orientation, which can rapidly change from voxel to voxel when the weights of the second and third orientation are similar. In Fig. 7ac, notice the mixture of left-right oriented fibers of the pons and the inferior-superior oriented motor pathways. In Fig. 6b, 7bd and 8bdf, notice the transition (from left to right) from one orientation (left-right fibers of the corpus callosum (CC)), to two orientations (superior-inferior fibers of the corticospinal tract (CST) and left-right fibers of the CC), to three orientations (superior-inferior fibers of the CST, anterior-posterior fibers of the superior longitudinal fasciculus (SLF) and left-right fibers of the CC), and back to two orientations (anterior-posterior fibers of the SLF and left-right fibers of the CC). Part of this transition can also be seen in Fig. 2.

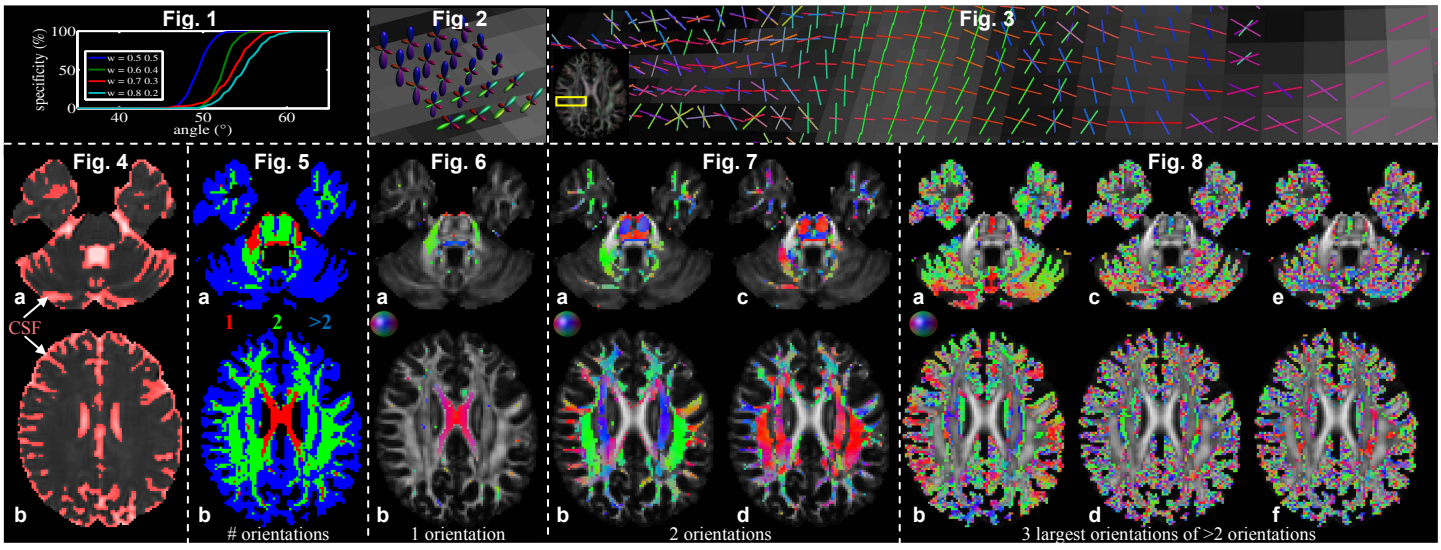

Conclusion: We showed that multiple-fiber CSD profiles arise consistently in various regions of the human brain where complex tissue structure is known to exist. Moreover, we detect voxels with more than two fiber orientations and detect a much higher proportion of multi-fiber voxels than previously reported.

References: [1] Alexander AL et al, MRM 45(5), 2001; [2] Tuch DS et al, MRM 48(4), 2002; [3] Frank LR, MRM 47(6), 2002; [4] Alexander DC et al, MRM 48(2), 2002; [5] Alexander DC, Ann NYAS 1064, 2006; [6] Behrens TEJ et al, NeuroImage 34(1), 2007; [7] Tournier JD et al, NeuroImage 35(4), 2007; [8] Chung S et al, NeuroImage 33(2), 2006; [9] Leemans A et al, MRM 62(6), 2009; [10] Otsu N, TSMC 9(1), 1979; [11] Leemans A et al, ISMRM, p. 3536, 2009.